Electronic Supplementary Information

Near-infrared absorbing non-fullerene acceptors with selenophene as π bridge for efficient organic solar cells

Ziqi Liang, [a, b] Miaomiao Li, *[a, b] Xiaomei Zhang, [a, b] Qi Wang, [a, b] Yu Jiang, [c] Hongkun Tian [c] and Yanhou Geng [a, b]

[a] School of Materials Science and Engineering and Tianjin Key Laboratory of Molecular Optoelectronic Science, Tianjin University, Tianjin 300072, P. R. China. E-mail: miaomiao.li@tju.edu.cn

[b] Collaborative Innovation Center of Chemical Science and Engineering (Tianjin), Tianjin University, Tianjin 300072, P. R. China.

[c] State Key Laboratory of Polymer Physics and Chemistry, Changchun Institute of Applied Chemistry, Chinese Academy of Sciences, Changchun, 130022, P. R. China.

Table of Contents

1. Instruments

^{1}H NMR and ^{13}C NMR spectra were measured at room temperature by a Bruker AV 400-MHz spectrometer with $CDCl_3$ as the solvent and tetramethylsilane (TMS) as internal standard. Matrix-assisted laser desorption ionization time-of-flight (MALDI-TOF) mass spectra were recorded on a Bruker/AutoflexIII Smartbean MALDI mass spectrometer with 2-[(2E)-3- (4-*tert*-buthylphenyl)-2-methylprop-2-enylidene]malononitrile (DCTB) as the matrix in a reflection mode. Elemental analysis was measured by a FlashEA1112 elemental analyzer. Thermogravimetric analysis (TGA) was conducted on Perkin-Elmer TGA-7 at a heating rate of 10 ºC/min under N_2 and differential scanning calorimetry (DSC) was performed by a Perkin-Elmer DSC7 thermal analyzer with a heating/cooling rate of ±10 °C/min under N_2. DFT calculation was carried out using Gaussian 09 with a hybrid B3LYP correlation functional and 6-31G (d) basis set, and all alkyl substituents were replaced with methyl groups in order to simplify the calculations. UV-*vis*-NIR absorption spectra were obtained on a Shimadzu UV-3600 Plus spectrometer. Film cyclic voltamograms (CV) were measured using a CHI660 electrochemical analyzer with a three-electrode cell at a scan rate of 100 mV/s in anhydrous acetonitrile (CH_3CN) with tetrabutylammonium hexafluorophosphate (Bu_4NPF_6, 0.1 mol/L) as the supporting electrolyte. A glassy carbon with 10 mm diameter, a Pt wire and a saturated calomel electrode (SCE) were used as working, counter and reference electrodes, respectively. The films were spin coated on the working electrode for CV measurements. E_{onset}^{ox} and E_{onset}^{re} are oxidation and reduction onsets, respectively, against the half potential of ferrocene/ferrocenium (Fc/Fc^+) (E^o = 0.39 V), as determined in CV curves. The HOMO and LUMO energy levels were estimated by the equations: HOMO = –(4.8+E_{onset}^{ox}) eV, LUMO =

–(4.8+E_{onset}^{re}) eV, respectively. The molecular weight of polymer PBDB-T was determined via high-temperature gel permeation chromatography (GPC) on a PL-GPC 220 system at 150 °C, with 1,2,4-trichlorobenzene as eluent and monodisperse polystyrene as standard. Atomic force microscopy (AFM) images were recorded in tapping mode on a Bruker MutiMode 8 atomic force microscope. Transmission electron microscopy (TEM) images were recorded on a JEM-1011 transmission electron microscope with accelerating voltage of 100 KV and camera length of 160 cm. Out-of-plane XRD was measured with a Bruker D8 Advance using CuKα radiation (λ= 1.54056 Å) and operated at 40 kV and 30 mA, and in-plane XRD was conducted on a Rigaku Smart Lab with CuKα source (λ= 1.54056 Å).

2. Fabrication and characterization of OSC devices

The devices with an architecture of glass/ITO/PEDOT:PSS (40 nm)/PBDB-T:acceptor /PDINO/Al (100 nm) were fabricated. The ITO coated glass substrates were cleaned ultrasonically with detergent, deionized water, acetone and isopropanol under ultrasonication for 15 min each. The dried ITO was treated with UV-ozone for 20 min, and then solution of PEDOT:PSS (Baytron P AI 4083) was spin-coated (ca. 40 nm thick) onto the surface. The substrates were then placed into an argon-filled glove box after being baked at 150 °C for 20 min. Subsequently, the active layer was spin-coated from donor (10 mg/mL) and acceptor (10 mg/mL) in CB solution for 60 s on the ITO/PEDOT:PSS substrate. The active layer thickness was measured using a Dektak150 profilometer. And then, PDINO, with CH_3OH as solvent (1 mg/mL), was spin-coated at 3000 rpm for 40 s on the active layers. Finally, a 100 nm nm Al layer was deposited on the PDINO layer under high vacuum (< 1.5×10^{-4} Pa). The effective area of each cell is 4 mm^2, as defined by masks for the solar cell devices. Keithley 2400 source

meter was used to measure *J-V* curves under 100 mW cm^{-2} AM 1.5G simulated solar light illumination provided by an AAA solar simulator (SS-F5-3A, Enli Technology Co. Ltd) calibrated with a standard photovoltaic cell equipped with a KG5 filter in a glove box. The EQE data were obtained using a solar cell spectral response measurement system (QE-R, Enli Technology Co. Ltd).

3. Fabrication and characterization of SCLC devices

Hole-only devices with an architecture of ITO/PEDOT:PSS (40 nm)/ PBDB-T:acceptor/Au (100 nm) and electron-only devices with an architecture of glass/Al (100 nm)/PBDB-T:acceptor/Al (100 nm) were fabricated. The devices were measured using Keithley 2400 source meter in a glove box under dark. The hole and electron mobilities were calculated by fitting the dark current using the Mott-Gurney relationship:

$$J = \frac{9}{8}\varepsilon_0\varepsilon_r\mu\frac{V^2}{L^3}$$

where J is the current density, L is the film thickness of the active layer, μ is the hole or electron mobility, ε_r is the relative dielectric constant of the transport medium, ε_0 is the permittivity of free space (8.85×10^{-12} F m^{-1}), V (= V_{appl} - V_{bi}) is the internal voltage in the device, where V_{appl} is the applied voltage to the device and V_{bi} is the built-in voltage due to the relative work function difference of the two electrodes.

4. Supplementary data

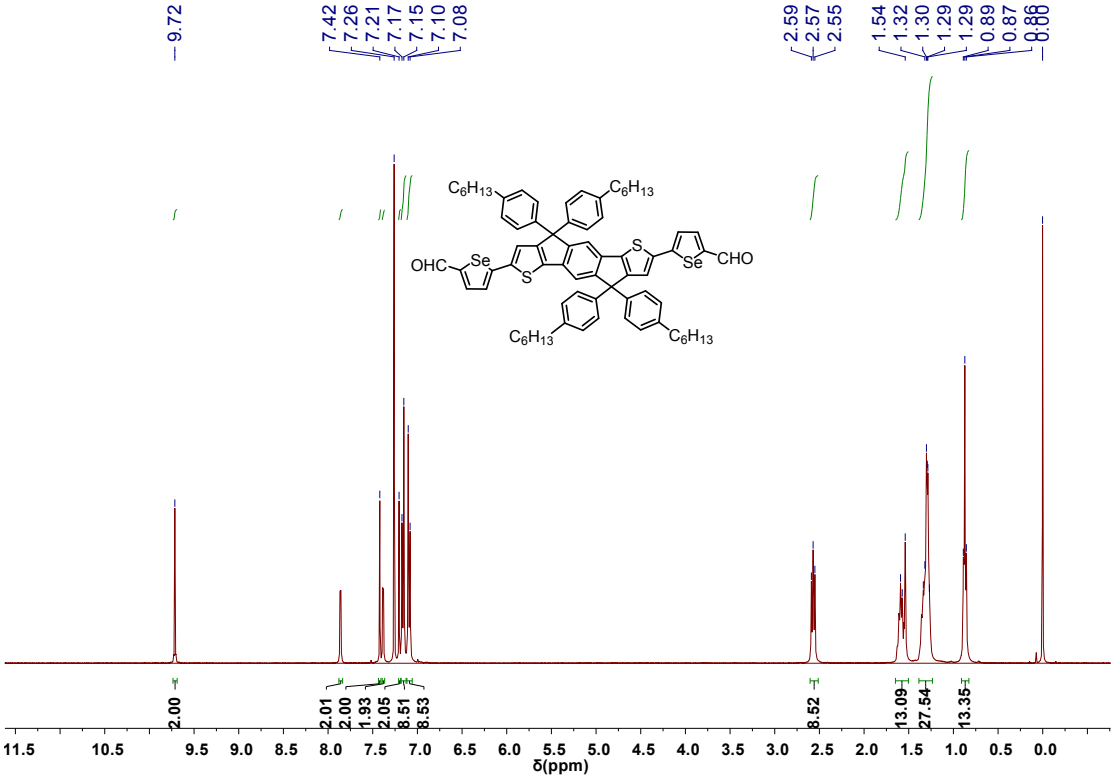

Fig. S1 ^{1}H NMR spectrum of compound **2**.

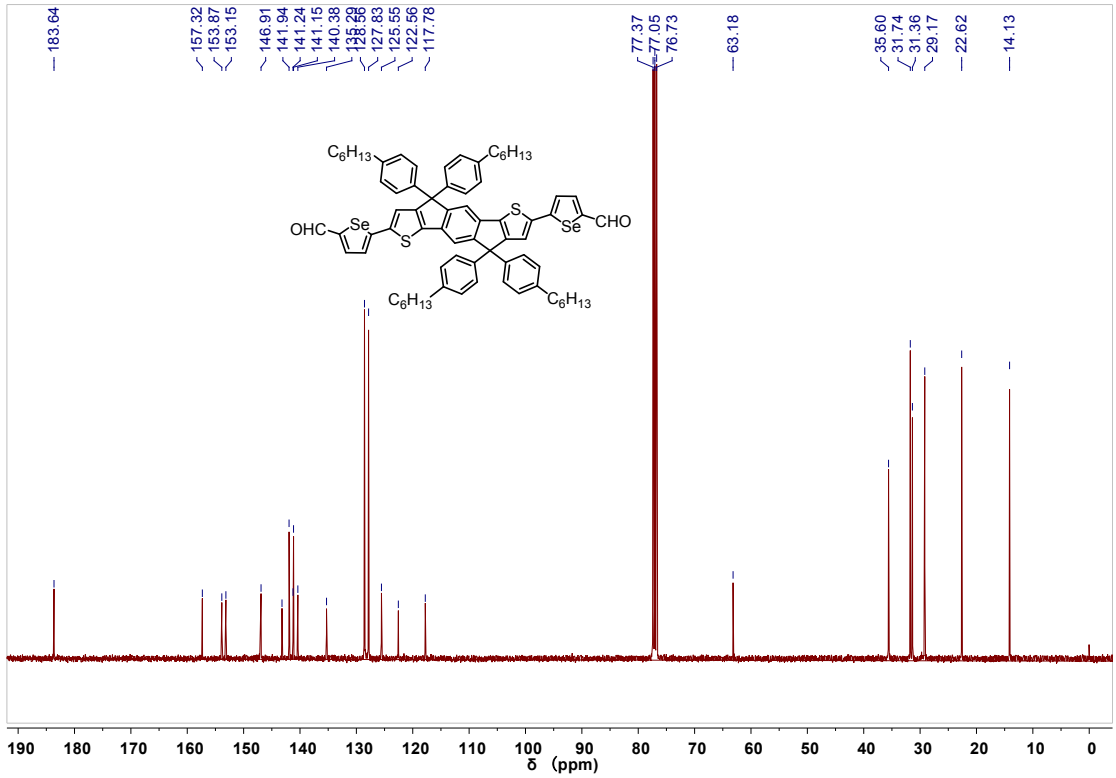

Fig. S2 ^{13}C NMR spectrum of compound **2**.

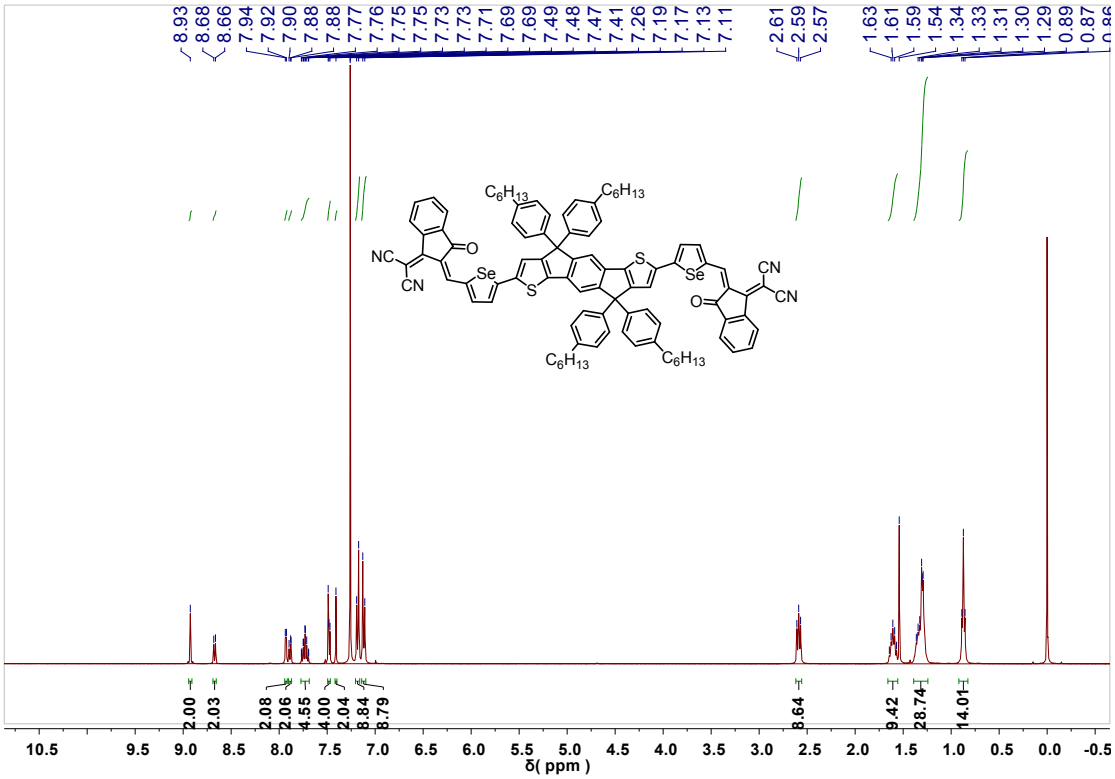

Fig. S3 ^{1}H NMR spectrum of **IDT2Se**.

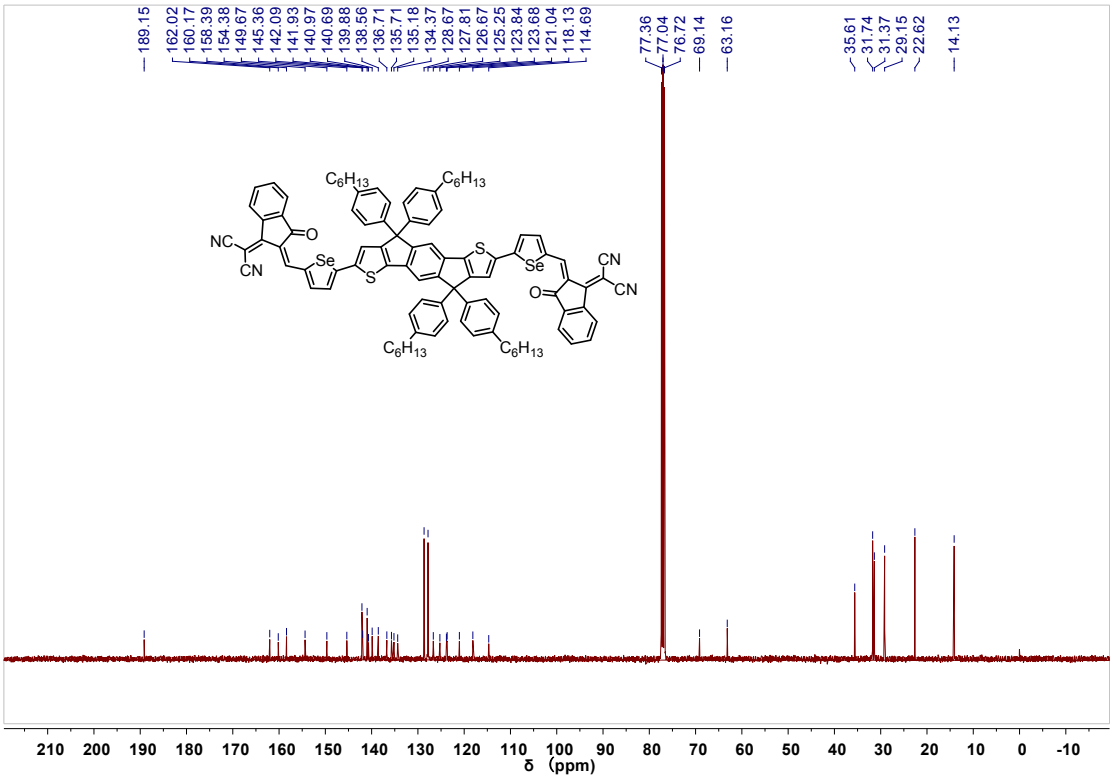

Fig. S4 ^{13}C NMR spectrum of **IDT2Se**.

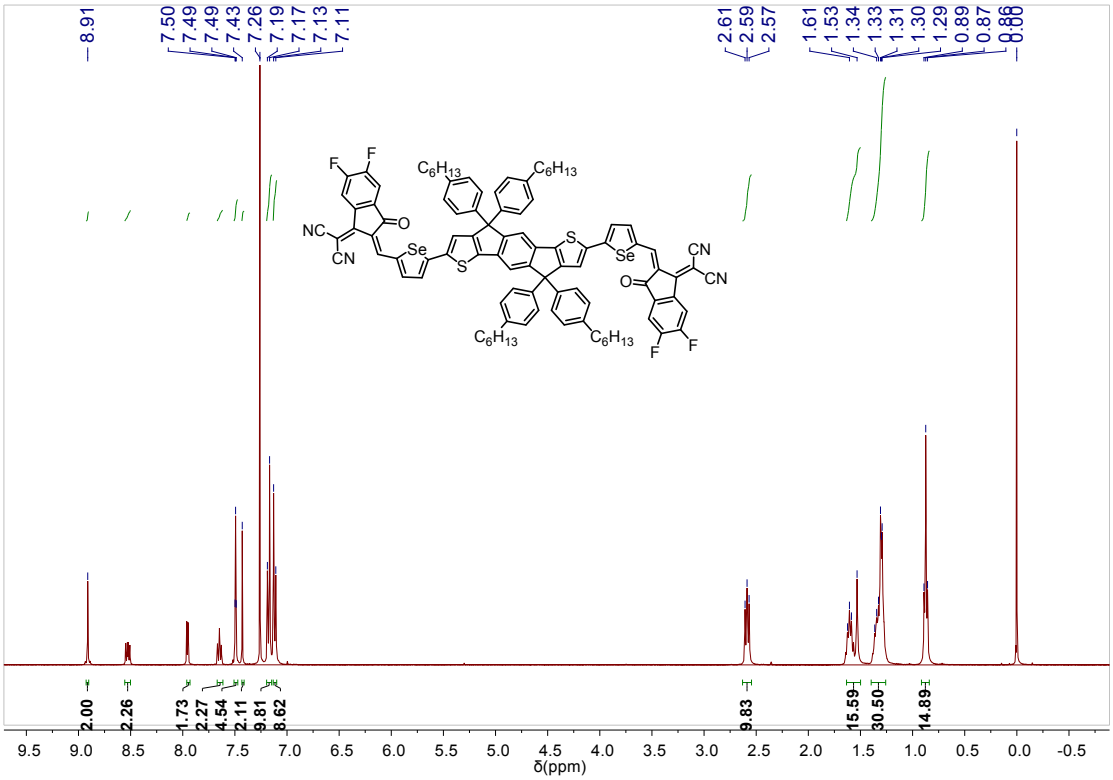

Fig. S5 ^{1}H NMR spectrum of **IDT2Se-4F**.

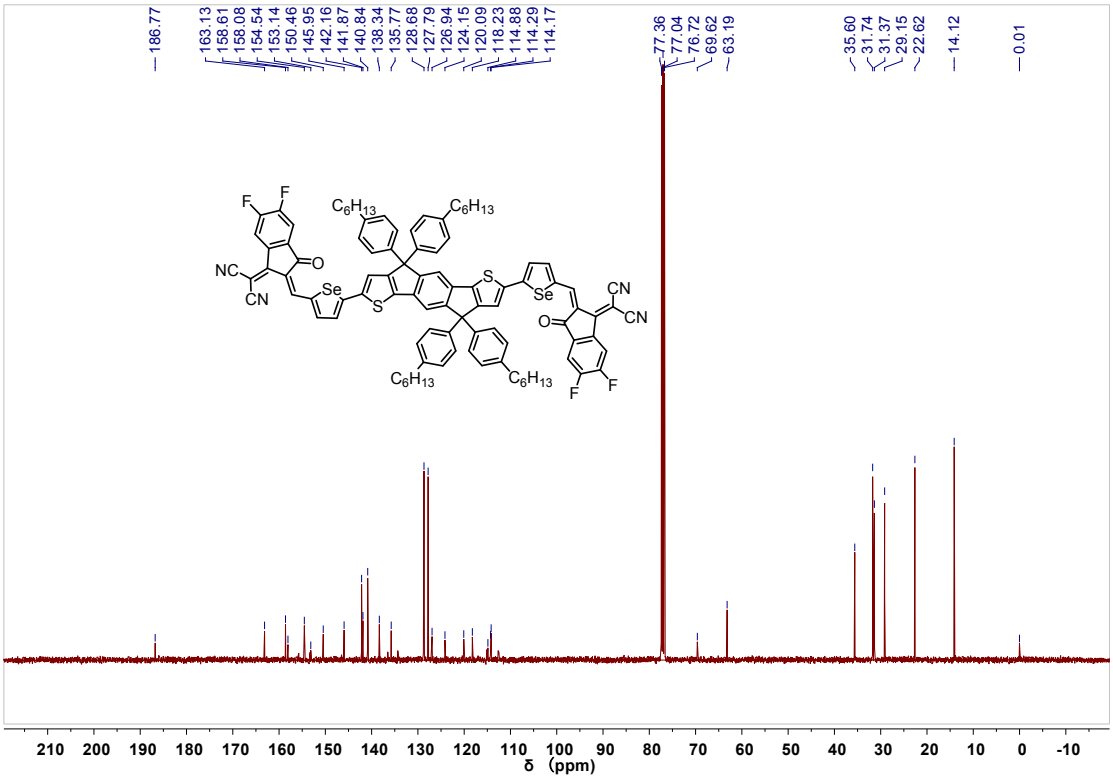

Fig. S6 ^{13}C NMR spectrum of **IDT2Se-4F**.

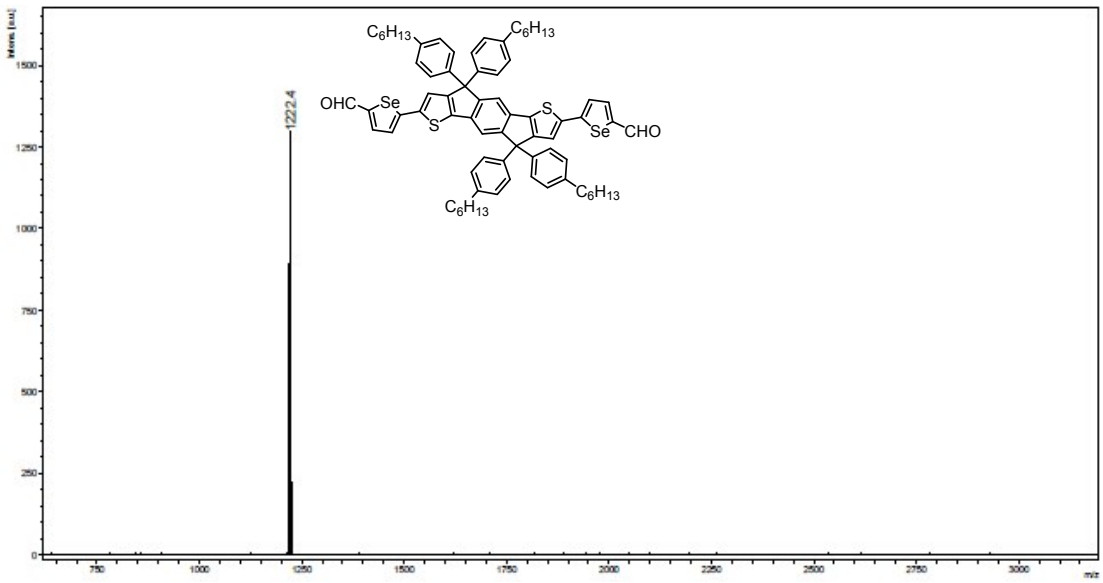

Fig. S7 The MALDI-TOF mass spectrum of compound **2**.

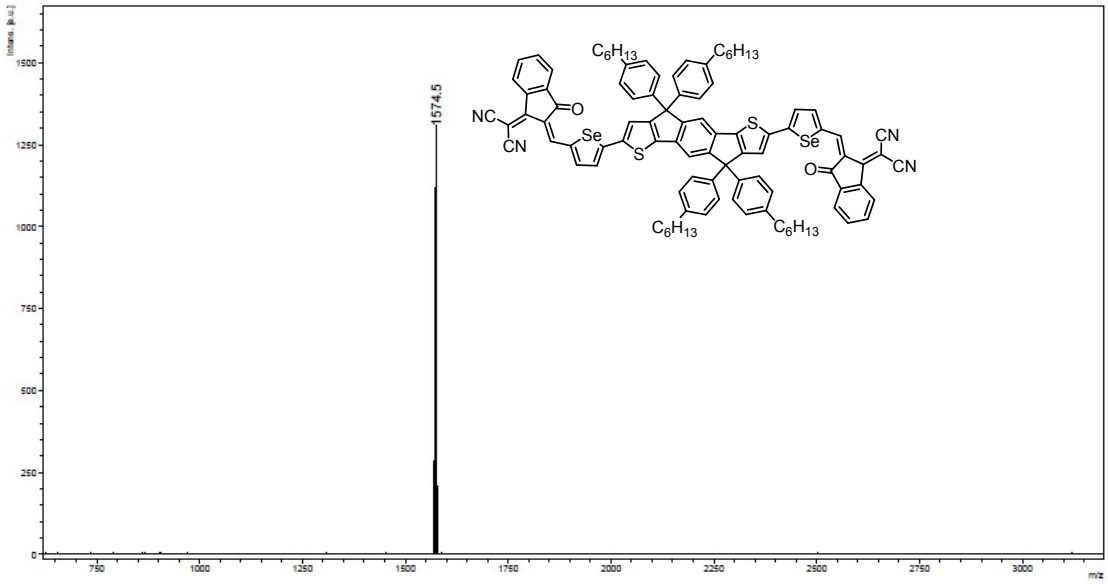

Fig. S8 The MALDI-TOF mass spectrum of **IDT2Se**.

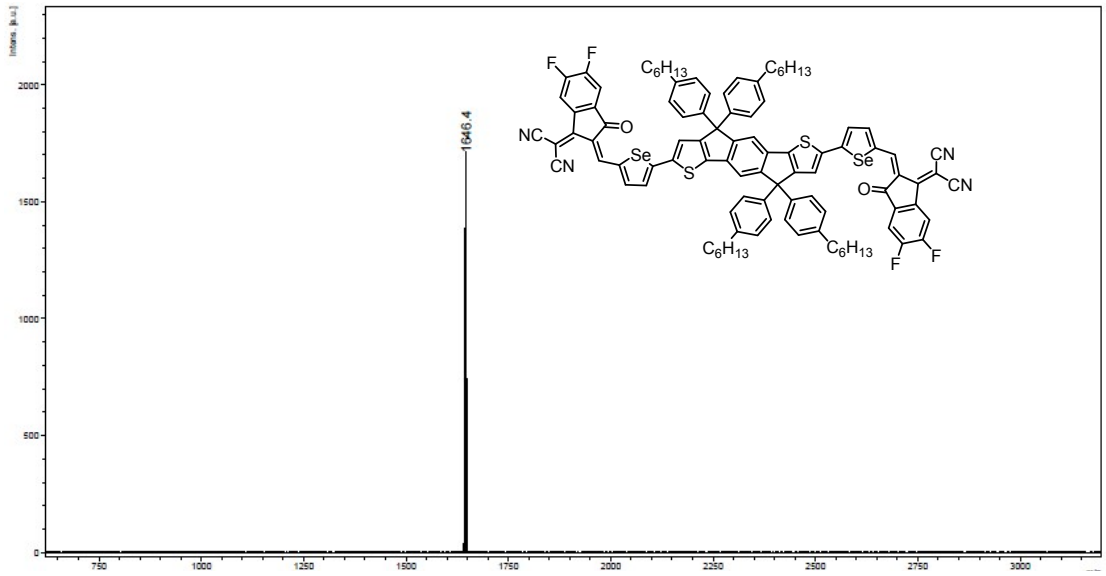

Fig. S9 The MALDI-TOF mass spectrum of **IDT2Se-4F**.

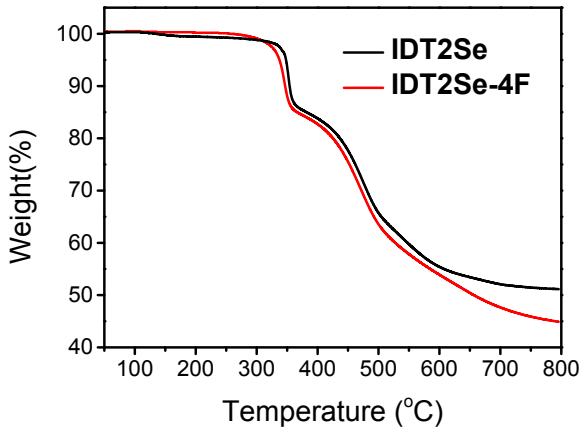

Fig. S10 TGA curves of **IDT2Se** and **IDT2Se-4F** in nitrogen with a heating rate of 10 °C/min.

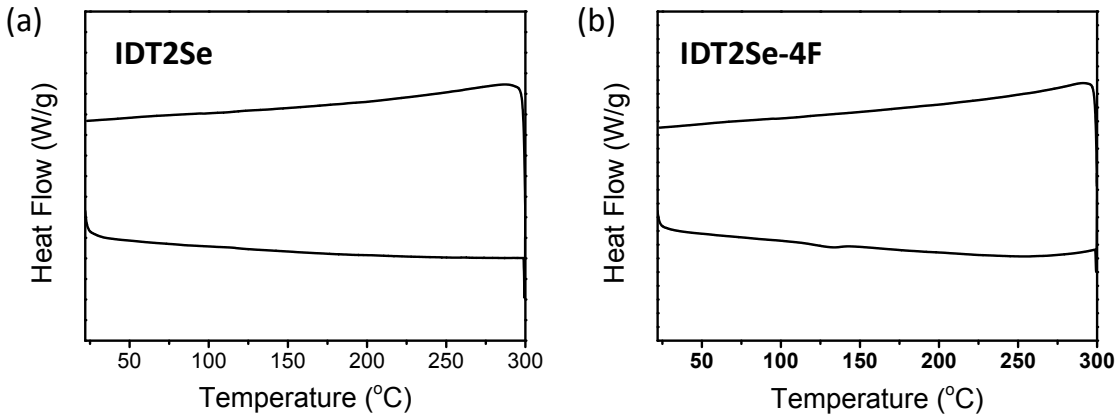

Fig. S11 The first cooling and the second heating DSC curves of **IDT2Se** and **IDT2Se-4F** in N_2 with a heating/cooling rate of 10 °C/min.

Table S1. Crystal data and structure refinement for **IDT2Se-4F**.[a]

Identification code	**IDT2Se-4F**	
Empirical formula	C98 H82 F4 N4 O2 S2 Se2	
Formula weight	1645.71	
Temperature	120.0(1) K	
Wavelength	0.71073 Å	
Crystal system	Monoclinic	
Space group	C2/c	
Unit cell dimensions	a = 31.859(7) Å	α= 90°.
	b = 16.153(4) Å	β= 94.79(3)°.
	c = 16.230(7) Å	γ = 90°.
Volume	8323(5) $Å^3$	
Z	4	
Density (calculated)	1.313 Mg/m^3	
Absorption coefficient	1.000 mm^{-1}	
F(000)	3400	
Crystal size	0.300 x 0.280 x 0.250 mm^3	
Theta range for data collection	3.141 to 25.009°.	
Index ranges	-33<=h<=37, -19<=k<=17, -19<=l<=19	
Reflections collected	26687	
Independent reflections	7330 [R(int) = 0.0993]	
Completeness to theta = 25.009°	99.8 %	
Absorption correction	Semi-empirical from equivalents	
Max. and min. transmission	1.00000 and 0.62411	
Refinement method	Full-matrix least-squares on F^2	
Data / restraints / parameters	7330 / 43 / 506	
Goodness-of-fit on F^2	1.027	
Final R indices [I>2sigma(I)]	R1 = 0.1058, wR2 = 0.2630	
R indices (all data)	R1 = 0.2002, wR2 = 0.3438	
Extinction coefficient	n/a	
Largest diff. peak and hole	1.828 and -0.618 $e.Å^{-3}$	

[a] CCDC number: 1818833

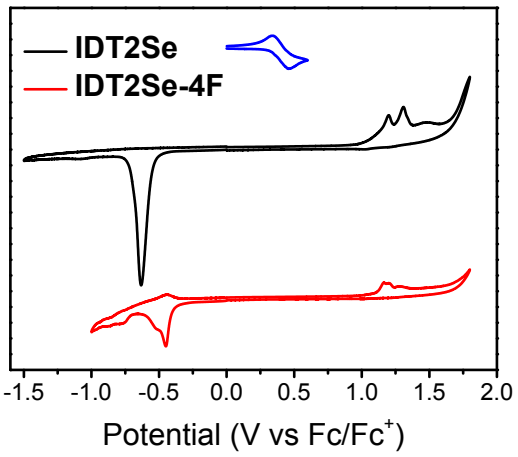

Fig. S12 Thin film cyclic voltammograms (CV) of **IDT2Se** and **IDT2Se-4F**.

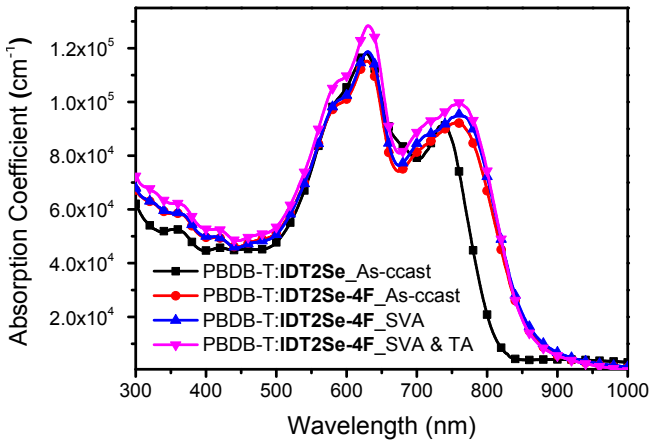

Fig. S13 Absorption spectra of PBDB-T:**IDT2Se** and PBDB-T:**IDT2Se-4F** blend films with different treatments. Donor:acceptor weight ratio: 1:1.

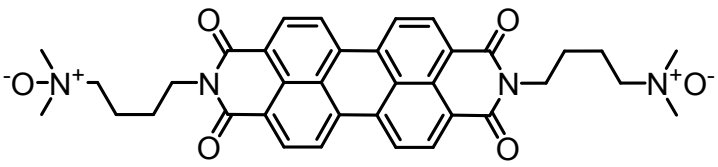

Fig. S14 Chemical structure of PDINO.

Table S2. The detailed photovoltaic performances of OSCs based on PBDB-T:**IDT2Se** and PBDB-T:**IDT2Se-4F** with different D:A ratio (wt:wt). The active layer thickness is ~110 nm. [a]

Acceptor	D:A ratio	V_{oc} (V)	J_{sc} (mA/cm^2)	FF (%)	PCE (%)
IDT2Se	1:0.8	0.89±0.01 (0.89)	16.69±0.25 (16.89)	57.5±1.0 (58.3)	8.54±0.22 (8.76)
	1:1	0.89±0.01 (0.89)	17.05±0.25 (17.08)	58.0±0.9 (58.6)	8.80±0.19 (8.91)
	1:1.2	0.89±0.01 (0.89)	17.62±0.23 (17.78)	55.1±0.9 (55.7)	8.64±0.18 (8.82)
IDT2Se-4F	1:0.8	0.81±0.01 (0.82)	18.77±0.31 (19.08)	61.7±1.2 (62.3)	9.38±0.37 (9.75)
	1:1	0.81±0.01 (0.81)	19.18±0.15 (19.28)	62.3±1.0 (63.0)	9.68± 0.16(9.84)
	1:1.2	0.81±0.01 (0.81)	20.01±0.35 (20.39)	58.6±0.9 (59.1)	9.50±0.26 (9.76)

[a] Statistical and optimal results are listed outside of parentheses and in parentheses, respectively. The average values are obtained from over 15 devices.

Table S3. The detailed photovoltaic performances of OSCs based on PBDB-T:**IDT2Se** and PBDB-T:**IDT2Se-4F** with different active layer thickness. The D:A ratio (wt:wt) is 1:1. [a]

Acceptor	Thickness (nm)	V_{oc} (V)	J_{sc} (mA/cm^2)	FF (%)	PCE (%)
IDT2Se	80	0.89±0.01 (0.89)	16.00±0.32 (16.17)	60.0±1.0 (61.0)	8.54±0.24 (8.78)
	110	0.89±0.01 (0.89)	17.05±0.25 (17.08)	58.0±0.9 (58.6)	8.80±0.19 (8.91)
	130	0.89±0.01 (0.89)	16.51±0.19 (16.58)	57.1±1.0 (57.8)	8.39±0.14 (8.53)
IDT2Se-4F	80	0.81±0.01 (0.81)	18.24±0.0.30 (18.53)	63.8±0.8 (64.6)	9.43±0.27 (9.70)
	110	0.81±0.01 (0.81)	19.18±0.15 (19.28)	62.3±1.0 (63.0)	9.68± 0.16(9.84)
	130	0.81±0.01 (0.81)	18.72±0.34 (19.03)	60.1±1.2 (61.3)	9.11±0.34 (9.45)

[a] Statistical and optimal results are listed outside of parentheses and in parentheses, respectively. The average values are obtained from over 15 devices.

Table S4. The detailed photovoltaic performances of OSCs based on PBDB-T:**IDT2Se** and PBDB-T:**IDT2Se-4F** with different treatments. The active layer thickness is ~110 nm, and the D:A ratio (wt:wt) is 1:1. [a]

Acceptor	Treatment		V_{oc}	J_{sc}	FF	PCE
	SVA	TA	(V)	(mA/cm^2)	(%)	(%)
IDT2Se	w/o	w/o	0.89±0.01 (0.89)	17.05±0.25 (17.08)	58.0±0.9 (58.6)	8.80±0.19 (8.91)
	60 s	w/o	0.89±0.01 (0.89)	17.09±0.24 (17.18)	58.5±1.0 (59.5)	8.90±0.20 (9.10)
	90 s	w/o	0.89±0.01 (0.89)	17.20±0.21 (17.31)	58.8±1.1 (59.9)	9.00±0.23 (9.23)
	120 s	w/o	0.88±0.01(0.88)	17.20± 0.30 (17.26)	58.6±0.8 (59.7)	8.87±0.20 (9.07)
	90 s	80 °C	0.88±0.01 (0.89)	17.31±0.20 (17.49)	59.8±1.0 (60.8)	9.11±0.25 (9.36)
	90 s	100 °C	0.88±0.01 (0.89)	17.25±34 (17.59)	59.4±1.2 (60.2)	9.02±0.30 (9.32)
IDT2Se-4F	w/o	w/o	0.81±0.01 (0.81)	19.18±0.15 (19.28)	62.3±1.0 (63.0)	9.68± 0.16(9.84)
	60 s	w/o	0.81±0.01 (0.81)	19.91±0.27 (20.00)	63.0±1.3 (64.0)	10.16±0.21 (10.37)
	90 s	w/o	0.80±0.01 (0.80)	20.52±0.23 (20.75)	64.0±1.2 (64.8)	10.50±0.26 (10.76)
	120 s	w/o	0.80±0.01 (0.80)	20.48±0.36 (20.60)	63.9±1.4 (65.0)	10.47±0.24 (10.71)
	90 s	80 °C	0.79±0.01 (0.79)	21.35±0.27 (21.49)	65.4±0.9 (65.9)	11.03±0.16 (11.19)
	90 s	100 °C	0.79±0.01 (0.79)	21.00±0.50 (21.47)	64.1±0.8 (64.8)	10.63±0.36 (10.99)

[a] Statistical and optimal results are listed outside of parentheses and in parentheses, respectively. The average values are obtained from over 15 devices.

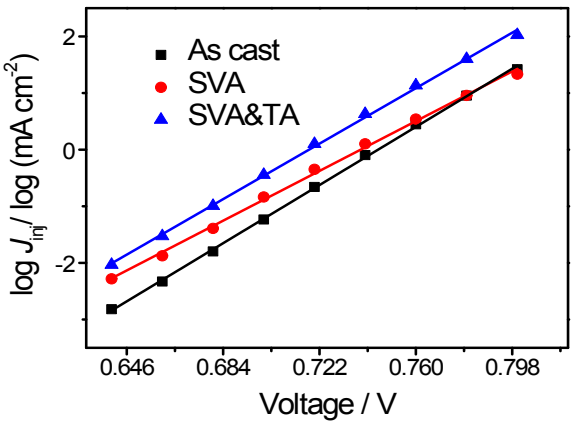

Fig. S15. The fitted dark injected current (J_{inj}) versus voltage (V) for the devices based on PBDB-T:**IDT2Se-4F** blend films with different treatment. [a]

[a] The dark injected current J_{inj} versus applied voltage for PBDB-T:**IDT2Se-4F** based devices was exponentially fitted according to Equation S1, therefore to determine reverse saturation current density $J_{0,n}$.

$$J_{inj} = J_{0,n} \exp(\frac{qV}{nkT})$$ Equation S1[1, 2]

Table S5. Measured and simulated performance parameters of the devices based on PBDB-T:**IDT2Se-4F** blend films with different treatments according to the dark J_{inj}-V curves.[a]

Treatment	V_{oc}/V	$J_{0,n}$/ mA cm^{-2}	nkT/q	J_{so} / mA cm^{-2}
As cast	0.81	1.79×10^{-9}	0.0370	7.65×10^{-2}
SVA	0.80	3.86×10^{-8}	0.0432	1.31×10^{-1}
SVA and TA	0.79	9.15×10^{-9}	0.0388	1.74×10^{-1}

[a] J_{so} is calculated according to Equation 2.

$$J_{0,n} = J_{so} \exp(\frac{-\Delta E_{DA}}{2nkT})$$ Equation S2[2, 3]

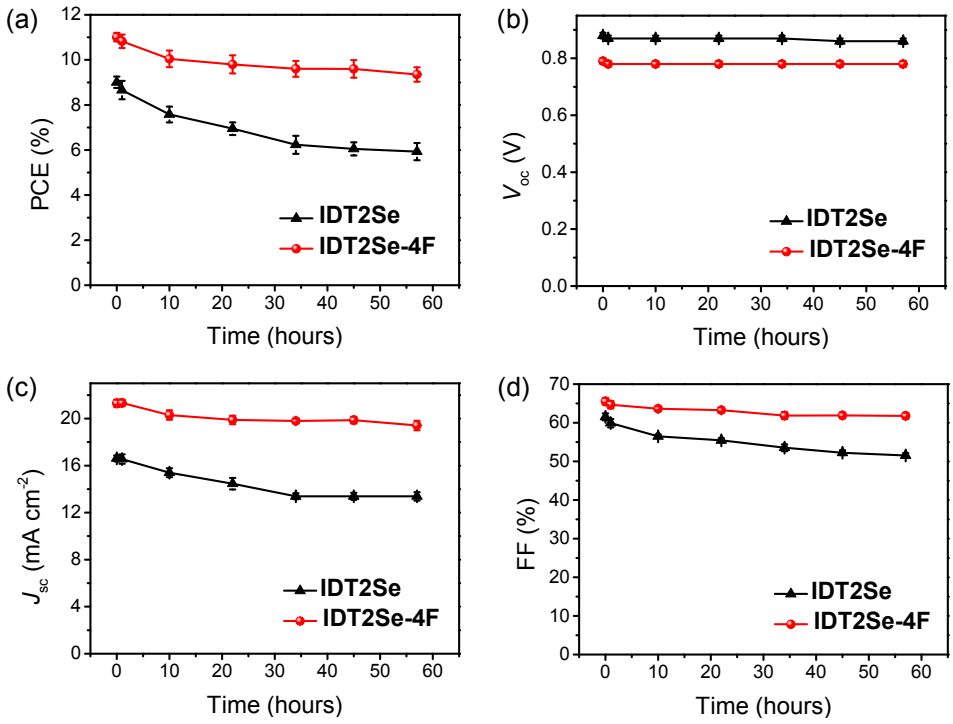

Fig. S16 Photovoltaic parameters versus continuous illumination (AM 1.5G, 100 mW/cm^2) time for PBDB-T:**IDT2Se** and PBDB-T:**IDT2Se-4F** based OSCs in an argon-filled glove box. The temperature of the devices under the lamp is around 50 ^{o}C. The error bars present standard deviations of at least ten devices averaged for each study.

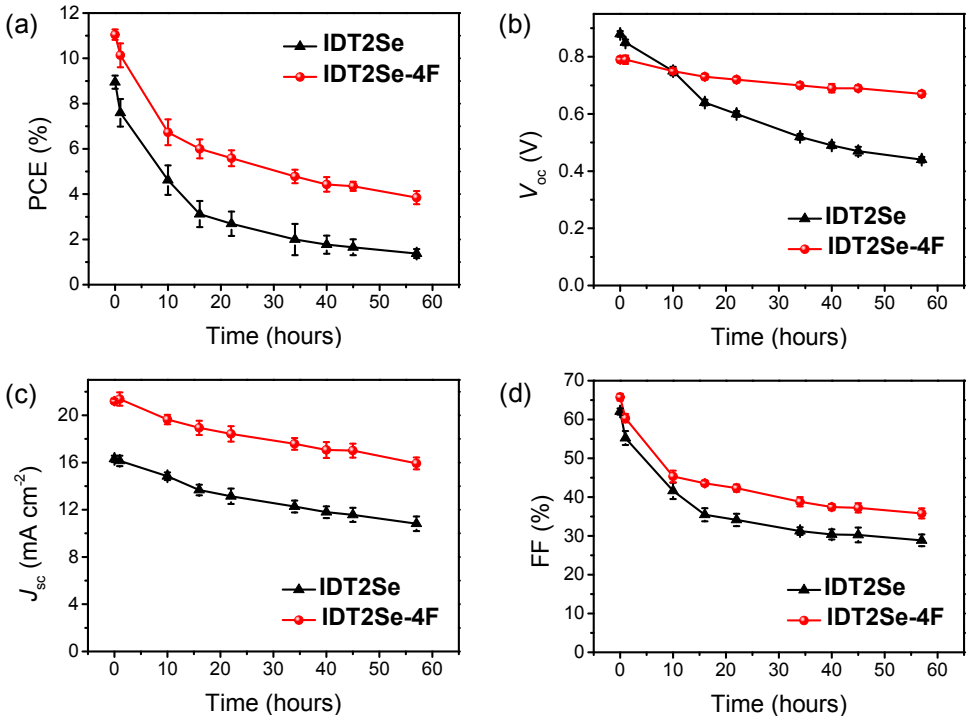

Fig. S17 Photovoltaic parameters versus continuous heating time for PBDB-T:**IDT2Se** and PBDB-T:**IDT2Se-4F** based OSCs at 100 °C in an argon-filled glove box. The error bars present standard deviations of at least ten devices averaged for each study.

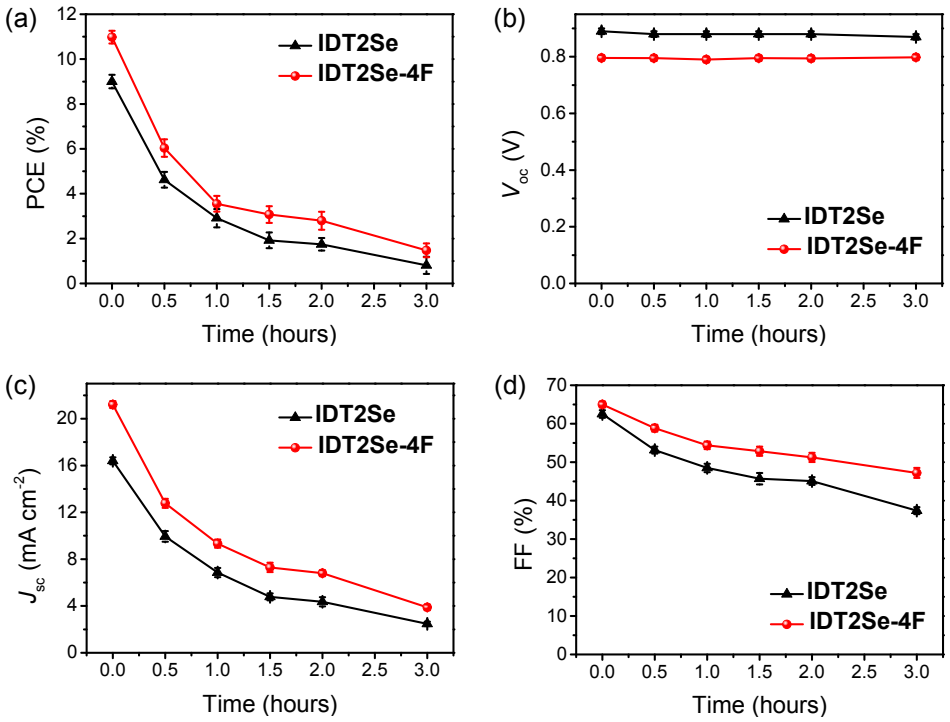

Fig. S18 Photovoltaic parameters versus exposure time in air (relative humidity: ~30%, room temperature: 25 °C) for PBDB-T:**IDT2Se** and PBDB-T:**IDT2Se-4F** based OSCs. The error bars present standard deviations of at least ten devices averaged for each study.

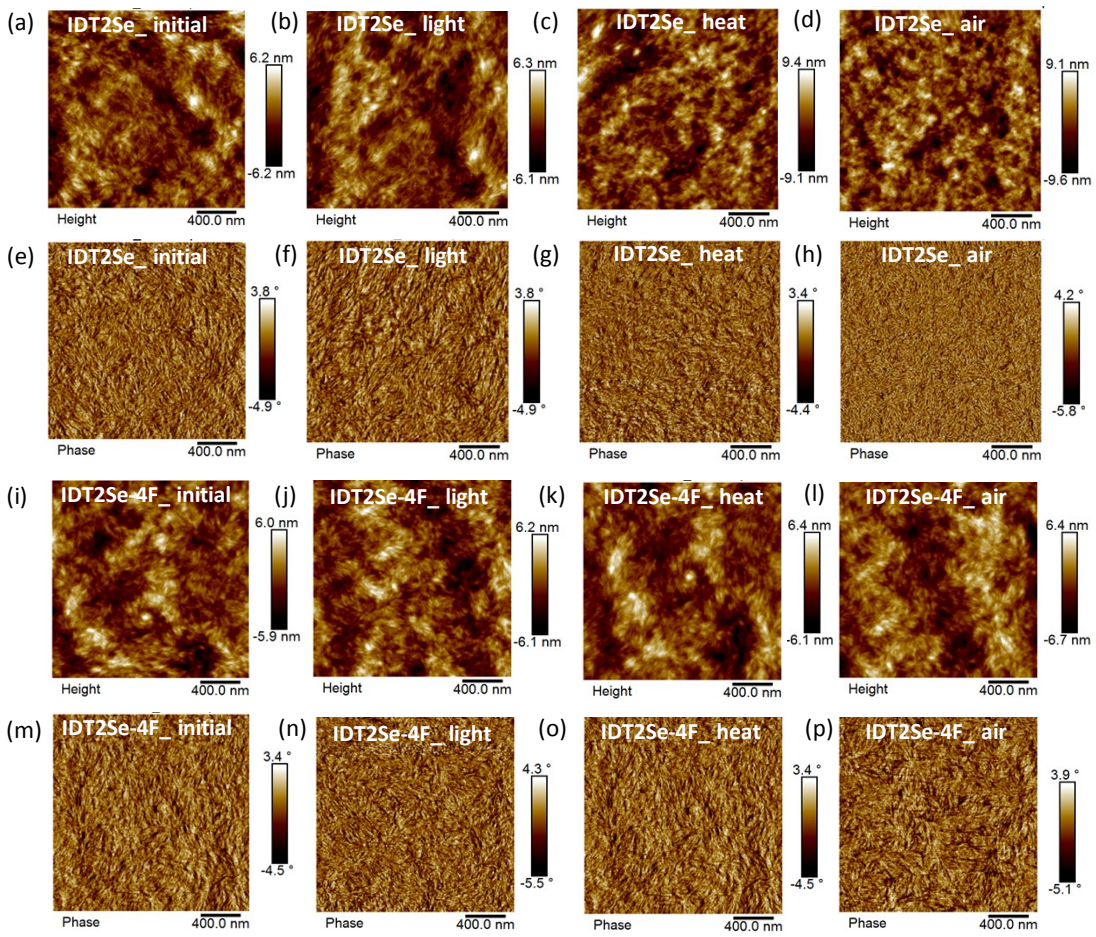

Fig. S19 AFM height (a-d, i-l) and phase images (e-h, m-p) of PBDB-T:**IDT2Se** (a-h) and PBDB-T:**IDT2Se-4F** (i-p) blend films after continuous illumination (b, f, j, n) and heating (c, g, k, o) for 57 h, and exposure in air (d, h, l, p) for 74 h.

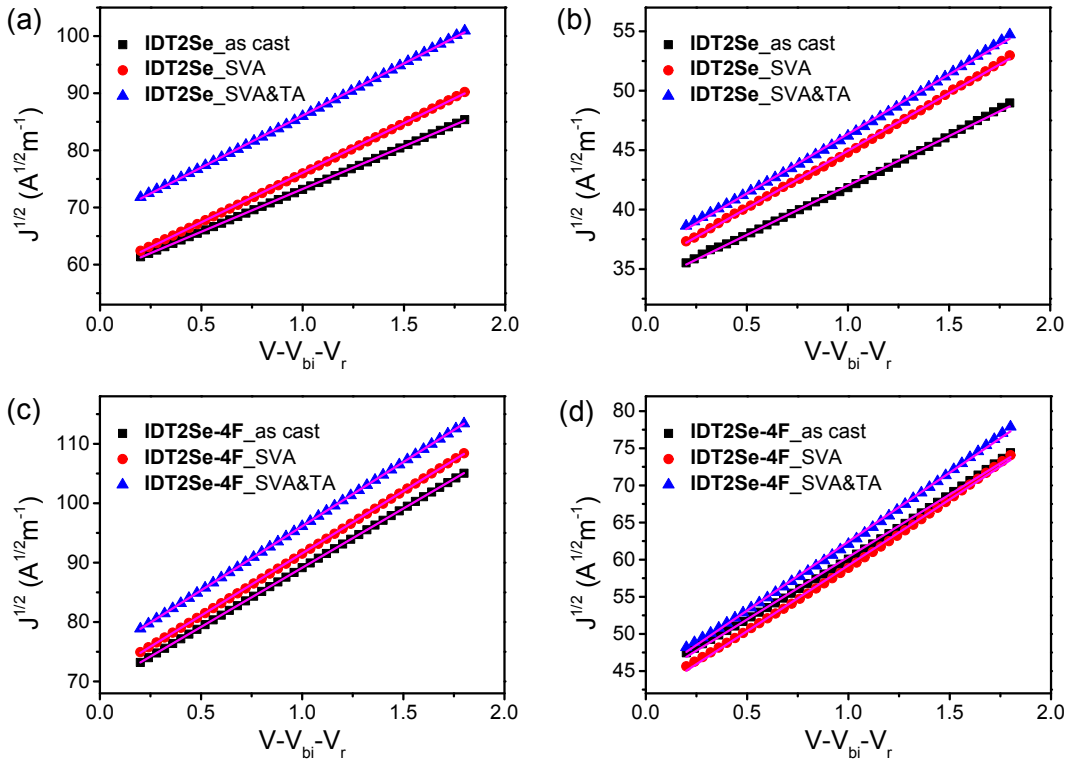

Fig. S20 *J-V* characteristics for the hole-only (a, c) and electron-only (b, d) devices fabricated with PBDB-T:**IDT2Se** (a, b) and PBDB-T:**IDT2Se-4F** (c, d). The solid lines represent the fit using a model of single carrier SCLC with field-independent mobility.

Table S6 Carriers mobility of PBDB-T:**IDT2Se** and PBDB-T:**IDT2Se-4F** blends measured by the space charge limited current (SCLC) method.

Blend film	Treatments	μ_h ($cm^2V^{-1}s^{-1}$)	μ_e ($cm^2V^{-1}s^{-1}$)	μ_h/μ_e
PBDB-T:**IDT2Se**	As cast	1.02	0.33	3.09
	SVA	1.38	0.44	3.14
	SVA and TA	1.52	0.48	3.17
PBDB-T:**IDT2Se-4F**	As cast	1.76	1.34	1.31
	SVA	1.97	1.50	1.31
	SVA and TA	2.08	1.64	1.27

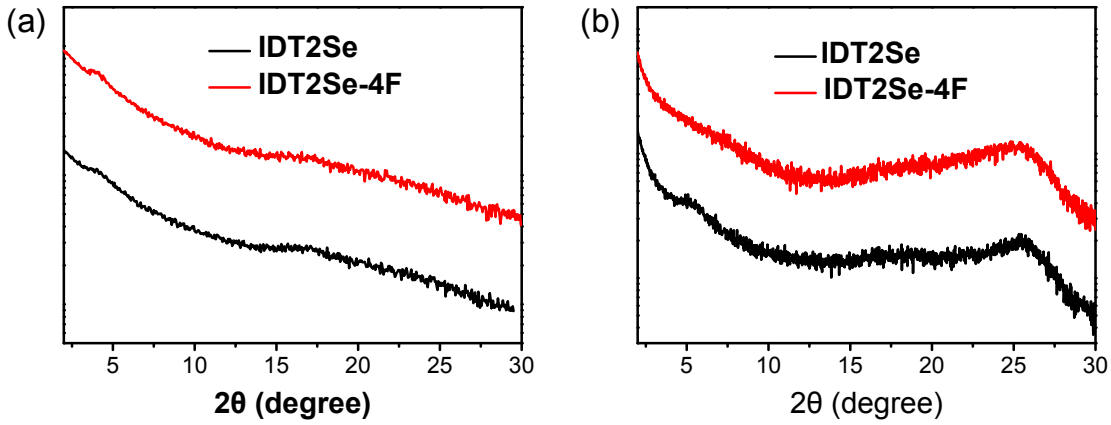

Fig. S21 In-plane (a) and out-of-plane (b) XRD patterns of **IDT2Se** and **IDT2Se-4F** neat films.

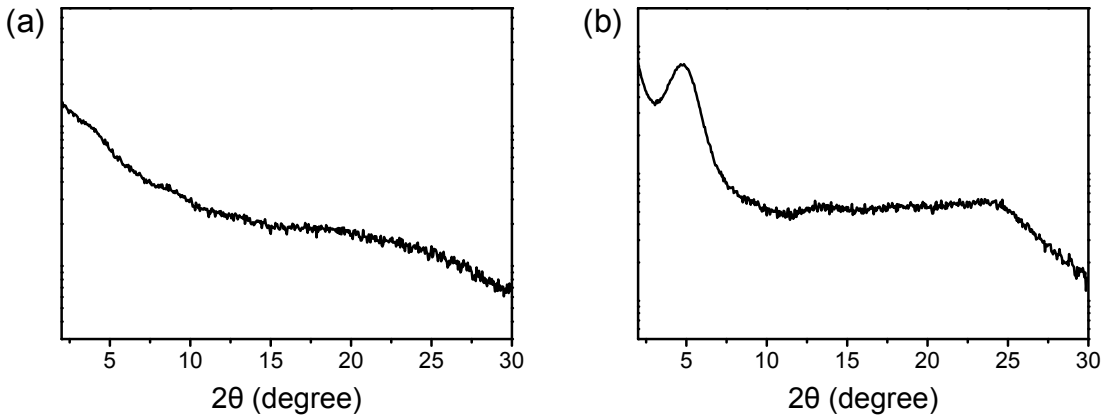

Fig. S22 In-plane (a) and out-of-plane (b) XRD patterns of PBDB-T neat films.

References

1 K. Vandewal, K. Tvingstedt, A. Gadisa, O. Inganas, J. V. Manca, *Nat. Mater.*, 2009, **8**, 904.

2 G. Long, X. Wan, B. Kan, Y. Liu, G. He, Z. Li, Y. Zhang, Y. Zhang, Q. Zhang, M. Zhang, Y. Chen, *Adv. Energy Mater.*, 2013, **3**, 639.

3 C. W. Schlenker, M. E. Thompson, *Chem. Commun.*, 2011, **47**, 3702.